ELSEVIER

Journal of Organometallic Chemistry 643–644 (2002) 468–478

Journal of Organometallic Chemistry

www.elsevier.com/locate/jorganchem

σ-Metathesis reaction and E–H activation (E = P, As) of diphosphanyl- and diarsanylsilanes in the presence of the metal complex fragments [(dppe)M] (M = Ni, Pd, Pt; dppe = 1,2-$(Ph_2P)_2C_2H_4$)

Matthias Driess [a,*], Felix Franke, Hans Pritzkow [b]

[a] *Lehrstuhl für Anorganische Chemie I: Molekül- und Koordinationschemie, Fakultät für Chemie der Ruhr-Universität, Universitätsstrasse 150, D-44801 Bochum, Germany*

[b] *Anorganisch-chemisches Institut der Universität, Im Neuenheimer Feld 270, D-69120 Heidelberg, Germany*

Received 27 August 2001; accepted 3 October 2001

Dedicated to Professor F. Mathey on the occasion of his 65th birthday

Abstract

The synthesis of the first 1-metalla-2,4-diphospha-3-silacyclobutanes [(dppe)M$(PH)_2$Si*t*-Bu(Is)] **1a** (M = Ni, Is = 2,4,6-triisopropylphenyl, dppe = 1,2-bis(diphenylphosphino)ethane), **1c** (M = Pd), **1d** (M = Pt) and the analogous 1-nickela-2,4-diarsa-3-silacyclobutane [(dppe)Ni$(AsH)_2$Si*t*-Bu(Is)] (**1b**) is reported, which was achieved by salt metathesis reaction of *t*-Bu(Is)Si$(EHLi)_2$ (**2a**, E = P; **2b**, E = As) with the respective metal chlorides [(dppe)MCl_2] in toluene at −70 °C. They were characterized by means of multinuclear NMR spectroscopy, mass spectrometry and combustion analysis. Their variable temperature ^{1}H- and ^{31}P-NMR spectra are in accordance with fast ring inversion processes and inversion of configuration at the E atoms (E = P, As), suggesting the presence of different diastereomeric forms in solution. The structures of the main diastereomeric form of **1a** (triclinic, $P\bar{1}$) and of the isotypic derivatives **1c** and **1d** (monoclinic, $P2_1/c$), respectively, were determined by X-ray diffraction analyses. The latter revealed all *cis* oriented E–H and *t*-Bu–Si bonds and puckered ME_2Si rings. Upon heating of **1a** and **1b** in toluene, the first 1-metalla-2,4-diphospha-3-silabicyclo[1.1.0]butane **3a** and its arsenic analogue **3b** was formed through intramolecular dehydrogenation reaction and were isolated in the form of orange crystals in 60 and 85% yield, respectively. The latter exist in the two diastereomeric forms (*t*-Bu)endo-**3a**, (*t*-Bu)exo-**3a** (molar ratio 4:1) and (*t*-Bu)endo-**3b**, (*t*-Bu)exo-**3b**, respectively. Their structures were established by X-ray diffraction analysis which revealed normal P–P (2.231(1) Å) and As–As single bond distances (2.451(1) Å), suggesting that the Ni atom offsets most of the ring strain effects caused by the Si ring atom. In contrast to **1a** and **1b**, heating of **1c** (M = Pd) in toluene at 80 °C affords, under evolution of H_2, merely the first dipalladiphosphasilabicyclo[1.1.1]pentane (**4a**) which was isolated in the form of black crystals in 65% yield. The analogous nickel compound **4b** is accessible by the salt metathesis reaction of 1,3-dilithiated [(dppe)Ni$(PLi)_2$Si*t*-Bu(Is)] with [(dppe)$NiCl_2$] and was isolated in the form of red crystals in 79% yield. Both complexes **4a** and **4b** were structurally characterized by X-ray diffraction. Surprisingly, the Pt complex **1d** remains unchanged even after prolonged heating in boiling toluene.

Keywords: σ-Metathesis reaction; Bond activation; Phosphides; Arsanides; Metal complex fragments

1. Introduction

The influence of silicon as a framework atom on the ring strain in small cycles is considerably stronger than that of carbon [1]. In line with this, the larger ring strain of three- and four-membered silaheterocycles is caused by the reluctance of silicon to undergo s,p hybridization [2]. This leads, in butterfly-like tetrasilabicyclo[1.1.0]butanes, to unusual electronic features in which the Si–Si bridgehead bond possesses diradical character [3]. Not only that, as revealed by theoretical calculations, one of the most interesting features of

* Corresponding author.

E-mail address: matthias.driess@ac1.ruhr-uni-bochum.de (M. Driess).

0022-328X/02/$ - see front matter
PII: S0022-328X(01)01348-1

heterosilabicyclo[1.1.0]butanes is the existence of bond-stretch isomers, which differ primarily in the distance between the bridgehead atoms. Hence fragile bridgehead bonds are also observed in 1,3-diphospha-2,4-disilabicyclo[1.1.0]butanes and their arsenic analogues **I** which have E–E bridgehead distances about 6% longer than those in unstrained cyclic diphosphanes (2.22 Å) and diarsanes (2.35 Å), respectively [4]. However, substitution of the two peripheral diorganosilandiyl fragments R_2Si: in **I** by isovalent electronic transition metal complex fragments results in a drastic change of the character of the E–E bridgehead bond. In fact, the E–E distances in isostructural M_2E_2 complexes **II** (M = transition metal; E = P, As) are ca. 0.1–0.15 Å shorter than expected for normal E–E single bonds due to favorable σ-donor and π-acceptor M–E interactions, according to the Dewar–Chatt–Duncanson model (Scheme 1) [5].

The opposite electronic influence of the transition metal center in **II** compared to that of the Si atoms in **I** prompted us to prepare the first mixed SiE_2M heterocycles **A** and **B**, respectively. In line with this, we expected that the E–E bridgehead bond in the new type of hybridic compounds **A** is probably less fragile than in the respective 2,4-diphospha-1,3-disilabicyclo[1.1.0]butanes **I**. Interestingly, the latter liberate silanediyl fragments through heating which undergo insertion reaction into the E–E bridgehead bond of **I** [6]. This raised the question whether **A** could serve as an analogous transfer reagent of carbene-like silanediyl and/or metal complex fragments [X] ([X] = SiR_2, [M]) across the E–E bond in **A**, affording asterane-like complexes of the type **C** (Scheme 2).

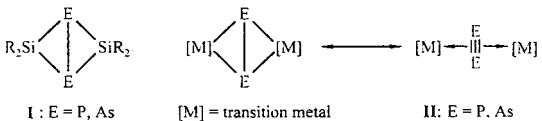

Scheme 1. Heterobicyclo[1.1.0]butane types **I** und **II**.

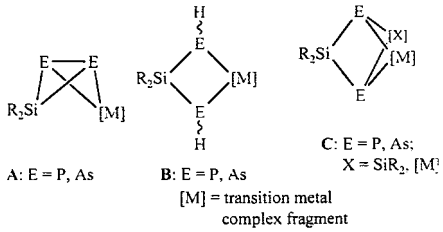

Scheme 2. Compound types **A**, **B** and **C**.

2. Experimental

2.1. General procedures

All manipulations with reagents, syntheses and spectroscopic measurements were carried out under anaerobic conditions in a Ar atmosphere. Solvents were purified by conventional methods and stored under an Ar atmosphere. The starting materials *tert*-butylisityldiphosphanylsilane (**2a**) and its arsenic analogue **2b** were prepared according to the literature [6,7]. The [(dppe)MCl_2] salts (M = Ni, Pd, Pt) were obtained by standard methods, using the respective $KMCl_3$ salts and dppe.

2.2. Physical measurements

^{1}H-NMR (300 MHz), ^{31}P-NMR (81 MHz) spectra were recorded in a Bruker WH300 spectrometer at room temperature (r.t.) unless otherwise stated. Chemical shifts (δ) are given relative to external standards (^{1}H: $SiMe_4$; ^{31}P: 85% aq. H_3PO_4). Mass spectra were recorded in a Finnigan MAT8230 spectrometer and all isolated compounds gave C,H combustion analyses consistent with their formulas.

2.3. Synthesis of the 3-tert-butyl-3-isityl-1-[1,2-bis(diphenylphosphino)ethane]-1-metalla-2,4-diphospha-3-silacyclobutanes (**1a**, **1c**, **1d**) and of 3-tert-butyl-3-isityl-1-[bis(diphenyl-phosphino)ethane]-1-metalla-2,4-diarsa-3-silacyclobutane (**1b**)

2.3.1. General synthetic procedure

A solution of 1.1 mmol of **2a** and **2b**, respectively, in 20 ml THF was treated with 1 ml of a 2.5 M solution of BuLi in hexane at 0 °C. The solution was allowed to warm up to r.t. and the solvent was removed in vacuo. The orange solid residue was taken up in 10 ml toluene and added to a suspension of 1.1 mmol of the respective [(dppe)MCl_2] complex (M = Ni, Pd, Pt) in 10 ml toluene at −78 °C. The mixture was warmed up to r.t. and stirred for 10 h. Subsequently, LiCl was filtered off and the orange–red solution was concentrated to ca. 10 ml and left for crystallization at r.t. Fractional crystallization affords the desired products in only moderate yields. The main products are the respective dehydrogenated compounds, that is, the heterobicyclo[1.1.0]butanes **3a**, **3b** or heterobicyclo[1.1.1]pentanes **4a**, **4b** (see below).

1a. Yield: 0.32 g (0.40 mmol, 36%), orange plates, m.p. 141–142 °C (dec.). ^{1}H-NMR (C_6D_6): δ = 1.35 (d, $^3J_{HH}$ = 7 Hz, 6H, *p*-CH(CH_3)$_2$); 1.42 (s, 9H, C(CH_3)$_3$), 1.46 (d,$^3J_{HH}$ = 6.4 Hz, 6H, *o*-CH(CH_3)$_2$), 1.66 (d,$^3J_{HH}$ = 7 Hz, 6H, *o*-CH(CH_3)$_2$), 1.98 (d, br, $^2J_{HH}$ = 16 Hz, 4H, PCH_2), 2.24 (s, CH_3 of solvate toluene), 2.91 (sept, $^3J_{HH}$ = 6.6 Hz, 1H, *p*-CH(CH$_3$)$_2$), 4.28 (sept,

$^3J_{HH} = 6.6$ Hz, 2H, *o*-C*H* ($CH_3)_2$), 7.25 (m, arom. H), 7.29 (m, arom. H), 7.78 (m, arom. H). ^{31}P-NMR (C_6D_6): $\delta = -190$ (br, *P*H), 51.3 (t, $J = 1/2|^2J_{PP,cis} + {}^2J_{PP,trans}| = 22.0$ Hz, dppe). EIMS; *m*/*z* (%): 806 ([M − 2H]$^+$, 17), 749 ([M − 2H − C($CH_3)_3$]$^+$, 10), 457 ([Ni(dppe)]$^+$, 10), 398 ([dppe]$^+$, 82), 353 ([M − dppe − C($CH_3)_3$]$^+$, 100). $C_{45}H_{58}NiP_4Si$ (809.6): Calc.: C, 66.76; H, 7.22. Anal. Found: C, 66.53; H, 7.20%.

1b. Yield: 0.46 g (0.45 mmol, 40.9%), orange plates, m.p. 154–155 °C (dec.). ^{1}H-NMR (C_6D_6): $\delta = 1.36$ (d, $^3J_{HH} = 7$ Hz, 6H, *p*-CH(C$H_3)_2$); 1.40 (s, 9H, C(C$H_3)_3$), 1.44 (d,$^3J_{HH} = 6.4$ Hz, 6H, *o*-CH(C$H_3)_2$), 1.69 (d,$^3J_{HH} = 7$ Hz, 6H, *o*-CH(C$H_3)_2$), 2.02 (d, br, $^2J_{HH} = 16$ Hz, 4H, PCH_2), 2.23 (s, CH_3 of solvate toluene), 3.04 (sept, $^3J_{HH} = 6.6$ Hz, 1H, *p*-C*H*($CH_3)_2$), 4.41 (sept, $^3J_{HH} = 6.6$ Hz, 2H, *o*-C*H* ($CH_3)_2$), 7.26 (m, arom. H), 7.31 (m, arom. H), 7.75 (m, arom. H). EIMS; *m*/*z* (%): 1019 ([M − 2H]$^+$, 11), 962 ([M − 2H − C($CH_3)_3$]$^+$, 9), 457 ([Ni(dppe)]$^+$, 10), 398 ([dppe]$^+$, 78), 575 ([M − dppe − C($CH_3)_3$]$^+$, 100). $C_{45}H_{58}As_2NiP_2Si$ (1022.6): Calc.: C, 52.85; H, 5.72. Anal. Found: C, 52.67; H, 5.69%.

1c. Yield: 0.26 g (0.30 mmol, 27%), yellow rhombic crystals, m.p. 170–175 °C (dec.). ^{1}H-NMR (C_6D_6): $\delta = 1.22$ (d, $^3J_{HH} = 7$ Hz, 6H, *p*-CH(C$H_3)_2$), 1.41 (s, 9H, C(C$H_3)_3$), 1.39 (s, 9H, C(C$H_3)_3$), 1.61 (br, 12H, *o*-CH(C$H_3)_2$), 1.9–2.1 (br, 4H, PCH_2), 2.77 (sept, $^3J_{HH} = 6.6$ Hz, 1H, *p*-C*H*($CH_3)_2$), 4.4 (br, 2H, *o*-C*H*($CH_3)_2$), 7.00 (m, arom. H), 7.56 (br, aromat. H), 7.77 (br, aromat. H). ^{31}P-NMR (C_6D_6): $\delta = -272$ (br, *P*H); −225 (br, *P*H), −216 (br, *P*H), 35–40 (br, m, *P*CH_2). EIMS; *m*/*z* (%): 854 ([M − 2H]$^+$, 48), 797 ([M − 2H − C($CH_3)_3$]$^+$, 58), 734 ([M − 2H − C_6H_5 − CH($CH_3)_2$]$^+$, 33), 504 ([Pd(dppe)]$^+$, 10), 398 ([dppe]$^+$, 60); 183 ([Ph_2P–2H]$^+$, 100). $C_{45}H_{58}P_4PdSi$ (857.3): Calc.: C, 63.05; H, 6.82; Anal. Found: C, 62.78; H, 6.77%.

1d. Yield: 0.52 g (0.55 mmol, 50%); yellow rhombic plates, m.p. 233–235 °C (dec.). ^{1}H-NMR (C_6D_6): $\delta = 1.21$ (d, $^3J_{HH} = 7$ Hz, 6H, *p*-CH(C$H_3)_2$), 1.39 (d,$^3J_{HH} = 6.6$ Hz, 6H, *o*-CH(C$H_3)_2$), 1.40 (s, 9H, C(C$H_3)_3$), 1.61 (d,$^3J_{HH} = 6.6$ Hz, 6H, *o*-CH(C$H_3)_2$), 1.95 (br, 4H, PCH_2), 2.90 (sept, $^3J_{HH} = 7$ Hz, 1H, *p*-C*H*($CH_3)_2$), 4.33 (br., 2H, *o*-C*H*($CH_3)_2$), 6.97 (m, 10H arom. H), 7.06 (td, 8H, $^3J_{HH} = 6$ Hz, $^4J_{HH} = 1.8$ Hz, arom. H), 7.78 (m, arom. H), 7.14 (s, 2H, arom. H of Is), 7.60 (pseudo t, $^2J_{PH} = 11$ Hz, $^3J_{HH} = 6$ Hz, arom. H), 7.82 (pseudo t, $^2J_{PH} = 11$ Hz, $^3J_{HH} = 6$ Hz, arom. H of PPh). ^{31}P-NMR (C_6D_6): $\delta = -211$ (br, *P*H), 44.2 (tm, $^1J_{PtP} = 1120$ Hz, *P*Ph), 43.2 (tm, $^1J_{PtP} = 1120$ Hz, *P*Ph). EIMS; *m*/*z* (%): 943 ([M − 2H]$^+$, 44), 887 ([M − 2H − C($CH_3)_3$]$^+$, 100), 825 ([M − 2H − C_6H_5 − CH($CH_3)_2$]$^+$, 33), 593 ([Pt(-dppe)]$^+$, 25), 398 ([dppe]$^+$, 82). $C_{45}H_{58}P_4PtSi$ (946.0): Calc.: C, 57.13; H, 6.18. Anal. Found: C, 56.84; H, 6.15%.

*2.4. Synthesis of 3-tert-butyl-3-isityl-1-[1,2-bis-(diphenylphosphino)ethane]-1-nickela-2,4-diphospha-3-silabicyclo[1.1.0]butane (**3a**) and 3-tert-butyl-3-isityl-1-[1,2-bis(diphenylphosphino)ethane]-1-nickela-2,4-diarsa-3-silabicyclo[1.1.0]butane (**3b**)*

3a. A solution of 0.43 g (1.10 mmol) of **2a** in 20 ml THF was treated with 1 ml of a 2.5 M solution of BuLi in hexane at 0 °C. The pale yellow solution was allowed to warm up to r.t. and the solvent was removed in vacuo. The yellow residue was taken up in 10 ml toluene and added to a suspension of 1.10 mmol of [(dppe)$NiCl_2$] in 10 ml toluene at 0 °C. The reaction mixture was warmed up to r.t. and stirred for 10 h. Subsequently, LiCl was filtered off and the deep brown solution was concentrated to ca. 10 ml and left for crystallization at r.t., resulting in a mixture of the (*t*-Bu)endo-**3a** and (*t*-Bu)exo-**3a** isomers. Yield: 0.48 g (0.60 mmol, 60%), orange solid; m.p. 181–184 °C (dec.). Single crystals of (*t*-Bu)endo-**3a** suitable for X-ray diffraction analysis result from concentrated benzene solutions at r.t. Alternatively, heating of solutions of **1a** for 12 h in boiling toluene affords also a mixture of endo, exo-**3a** in the ratio of ca. 4:1. ^{1}H-NMR (C_6D_6): $\delta = 0.75$ (s, C(C$H_3)_3$, (*t*-Bu)endo-**3a**), 1.12 (s, C(C$H_3)_3$, (*t*-Bu)exo-**3a**), 0.86, 1.34, 1.45, 1.51, 1.60, 1.83 (d,$^3J_{HH} = 7$ Hz, each set 3H, *o*-CH(C$H_3)_2$), 2.91 (sept, $^3J_{HH} = 6.6$ Hz, 1H, *p*-C*H*($CH_3)_2$), 4.60 (sept, $^3J_{HH} = 6.6$ Hz, 1H, *o*-C*H*($CH_3)_2$), 4.77 (sept, $^3J_{HH} = 6.6$ Hz, 1H, *o*-C*H*($CH_3)_2$); 6.96–7.35 (m, arom. H), 7.80 (m, arom. H), 7.97 (m, arom. H). ^{31}P-NMR (C_6D_6): $\delta = -82.9$ (pseudo-t, $J = 1/2|^2J_{PP,cis} + {}^2J_{PP,trans}| = 30.8$ Hz, *P*Si, (*t*-Bu)endo-**3a**), −73.8 (pseudo-t, $J = 1/2|^2J_{PP,cis} + {}^2J_{PP,trans}| = 32.4$ Hz, *P*Si, (*t*-Bu)exo-**3a**); 51.5 (pseudo-t, $J = 1/2|^2J_{PP,cis} + {}^2J_{PP,trans}| = 32.4$ Hz, *P*Ph, (*t*-Bu)endo-**3a**), 58.1 (pseudo-t, $J = 1/2|^2J_{PP,cis} + {}^2J_{PP,trans}| = 30.8$ Hz, *P*Ph, (*t*-Bu)exo-**3a**). EIMS; *m*/*z* (%): 806 ([M]$^+$, 17), 749 ([M − 2H − C($CH_3)_3$]$^+$, 10), 457 ([Ni(dppe)]$^+$, 10), 398 ([dppe]$^+$, 82), 353 ([M − dppe − C($CH_3)_3$]$^+$, 100). $C_{45}H_{56}NiP_4Si$ (807.6): Calc.: C, 66.92; H, 6.98. Anal. Found: C, 66.69; H, 6.90%.

3b. An exo, endo-isomer mixture of **3b** was synthesized and isolated similar to the procedure for **3a**, starting off from 1.12 g (1.10 mmol) **2b** and 1.10 mmol of [(dppe)$NiCl_2$]. Crystallization at r.t. affords a mixture of the expected endo, exo-isomers, (*t*-Bu)endo-**3b** and (*t*-Bu)exo-**3b**, in the ratio of 8:1 (^{1}H-NMR). Yield: 0.88 g (0.86 mmol, 78%), orange solid; m.p. 171–174 °C (dec.). Single crystals of (*t*-Bu)endo-**3b**, suitable for X-ray diffraction analysis, result from concentrated benzene solutions at r.t. ^{1}H-NMR (C_6D_6): $\delta = 0.70$ (s, C(C$H_3)_3$, (*t*-Bu)endo-3b), 1.19 (s, C(C$H_3)_3$, (*t*-Bu)exo-**3b**), 0.84, 1.38, 1.54, 1.59, 1.63, 1.87 (d,$^3J_{HH} = 7$ Hz, each set 3H, *o*-CH(C$H_3)_2$), 2.97 (sept, $^3J_{HH} = 6.6$ Hz, 1H, *p*-C*H*($CH_3)_2$), 4.58 (sept, $^3J_{HH} = 6.6$ Hz, 1H, *o*-C*H*($CH_3)_2$), 4.83 (sept, $^3J_{HH} = 6.6$ Hz, 1H, *o*-

C*H*(CH_3)$_2$); 6.97–7.35 (m, arom. H), 7.91 (m, arom. H), 7.95 (m, arom. H). EIMS; *m*/*z* (%): 895 ([M]$^+$, 14), 836([M − 2H − C(CH_3)$_3$]$^+$, 12), 457 ([Ni(dppe)]$^+$, 8), 440 ([M − dppe − C(CH_3)$_3$]$^+$, 100), 398 ([dppe]$^+$, 91). $C_{45}H_{56}As_2NiP_2Si$ (895.5): Calc.: C, 60.35; H, 6.30. Anal. Found: C, 60.05; H, 6.24%.

2.5. Synthesis of 3-tert-butyl-3-isityl-2,4-diphospha-1,5-bis[1,2-bis(diphenylphosphino)ethane]-1,5-dipallada-3-silabicyclo[1.1.1]pentane (**4a**) and 3-tert-butyl-3-isityl-2,4-diphospha-1,5-bis[1,2-bis(diphenylphosphino)-ethane]-1,5-dinickela-3-silabicyclo[1.1.1]pentane (**4b**)

4a. A solution of 0.43 g (1.10 mmol) of **2a** in 20 ml THF was treated with 1 ml of a 2.5 molar solution of BuLi in hexane at 0 °C. The pale yellow solution was allowed to warm up to r.t. and the solvent was removed in vacuo. The yellow residue was taken up in 10 ml toluene and added to a suspension of 1.10 mmol of [(dppe)$PdCl_2$] in 10 ml toluene at 0 °C. The reaction mixture was warmed up to r.t. and stirred for 10 h. Subsequently, LiCl was filtered off and the dark red solution was concentrated to ca. 10 ml. Crystallization at r.t. affords black rhombic plates of the toluene solvate but only in 25% yield. Alternatively, **4a** is accessible through thermolysis of **1c**: A solution of 1.10 mmol **1c** in 30 ml toluene is heated for 12 h at 80 °C, giving a deep red solution. After concentration of the latter to ca. 10 ml, the product crystallizes at r.t. in the form of a toluene solvate. Yield: 0.47 g (0.35 mmol, 65%); m.p. 191–195 °C (dec.). ^{1}H-NMR (C_6D_6): δ = 1.21 (d,$^3J_{HH}$ = 7 Hz, 6H, *p*-CH(CH_3)$_2$), 1.28 (s, 9H, C(CH_3)$_3$), 1.30 (d,$^3J_{HH}$ = 7 Hz, 6H, *o*-CH(CH_3)$_2$), 1.50 (d,$^3J_{HH}$ = 7 Hz, 6H, *o*-CH(CH_3)$_2$), 2.22 (s, CH_3 of solvate toluene), 2.80 (m, br, 1H, *p*-C*H*(CH_3)$_2$), 4.30 (t, $^3J_{HH}$ = 7 Hz, 2H, *o*-C*H*(CH_3)$_2$), 6.6–7.2 (m, arom. H), 7.3–8.1 (m, arom. H), 7. 97 (m, arom. H). ^{31}P-NMR (C_6D_6): δ = −80.0 (s, *P*Si), 19.7 (m, *P*Ph), 22.7 (m, *P*Ph). EIMS; *m*/*z* (%): 1145 ([M − C_2H_4 − PPh_2]$^+$, 19); 1088 ([M − C_2H_4 − PPh_2 − *t*-Bu]$^+$, 39), 855 ([M − Pd·dppe]$^+$, 41), 797 ([M − Pd(dppe) − *t*-Bu]$^+$, 43), 735 ([M − Pd(dppe) − Ph − *i*-Pr]$^+$, 32), 398 ([dppe]$^+$, 85), 183 [PPh_2–2H]$^+$, 100). $C_{71}H_{80}P_6Pd_2Si$ (1360.2): Calc.: C, 62.69; H, 5.93. Anal. Found: C, 62.45; H, 5.88%.

4b. A solution of 1.10 mmol **1a** in 20 ml THF was treated with 1 ml of a 2.5 M solution of BuLi in hexane at 0 °C. The clear red solution was allowed to warm up to r.t. and slowly added to a suspension of 1.10 mmol of [(dppe)$NiCl_2$] in 10 ml toluene at 0 °C. Subsequently, the reaction mixture was warmed up to r.t. and stirred for 10 h. LiCl was removed upon filtration and the dark red solution was concentrated to ca. 10 ml from which the product crystallizes as toluene solvate at r.t. in the form of dark red plates. Yield: 1.10 g (0.87 mmol, 79%); m.p. 187–190 °C (dec.). ^{1}H-NMR (C_6D_6): δ = 1.26 (d, $^3J_{HH}$ = 7 Hz, 6H, *p*-CH(CH_3)$_2$), 1.33 (s, 9H, C(CH_3)$_3$), 1.38 (d,$^3J_{HH}$ = 7 Hz, 6H, *o*-CH(CH_3)$_2$), 1.61 (d,$^3J_{HH}$ = 7 Hz, 6H, *o*-CH(CH_3)$_2$), 2.20 (s, CH_3 of solvate toluene), 2.86 (m, br, 1H, *p*-C*H*(CH_3)$_2$), 4.41 (t, $^3J_{HH}$ = 7 Hz, 2H, *o*-C*H*(CH_3)$_2$), 6.8–7.3 (m, arom. H), 7.4–8.1 (m, arom. H), 8.02 (m, arom. H). ^{31}P-NMR (C_6D_6): δ = −60.5 (s, *P*Si), 19.4 (m, *P*Ph), 23.7 (m, *P*Ph). EIMS; *m*/*z* (%): 1049 ([M − C_2H_4 − PPh_2]$^+$, 12); 992 ([M − C_2H_4 − PPh_2 − *t*-Bu]$^+$, 25), 806 ([M − Ni·dppe]$^+$, 33), 749 ([M − Ni(dppe) − *t*-Bu]$^+$, 46), 686 ([M − Ni(dppe) − Ph − *i*-Pr]$^+$, 21), 398 ([dppe]$^+$, 91), 183 [PPh_2–2H]$^+$, 100). $C_{71}H_{80}P_6Ni_2Si$ (1264.7): Calc.: C, 67.43; H, 6.37. Anal. Found: C, 67.12; H, 6.35%.

2.6. X-ray crystallographic studies of **1a**, **1c**, **1d**, **3a**, **3b**, **4a** and **4b**

Crystal data are compiled in Table 1. Intensity data were collected for **1a**, **1c**, **1d**, **3a**, **3b**, **4a** in a Siemens Stoe AED2 diffractometer (Mo–K_α radiation, λ = 0.71073 Å, ω-scan, T = −70 °C) and for **4b** in a Syntex R3 (Mo–K_α radiation, λ = 0.71073 Å, ω-scan, T = 22 °C). A semiempirical absorption correction was applied (ψ-scans). The structures were solved by direct methods and refined by full matrix least squares based on F^2 with all measured reflections. Non-hydrogen atoms were refined anisotropically. Hydrogen atoms were included in calculated positions (except the hydrogens at the P-atoms in **1a** and **1d**, which were located and refined). In **1c** one of the P-atoms is disordered over two positions. Some of the structures are isotypic: **1c** and **1d**, but not **1a**; **3a** and **3b**; **4a** and **4b**. All compounds except **1c** and **1d** crystallize with solvent molecules, **1a** with toluene, **3a**, **3b**, **4a** and **4b** with benzene.

3. Results and discussion

3.1. Synthesis of the metallasilacyclobutanes **1a**–**1d**

The sterically congested diphosphanyl- and diarsanylsilanes **2a** and **2b** [6,7] were employed as starting materials for the synthesis of the M(EH)$_2$Si-heterocyclobutanes **1a**–**d** and transformed in a two-step process. Thus, partial lithiation of the EH_2 moieties in **2a**,**b** with two molar equivalents BuLi and subsequent salt metathesis reaction with the [M(dppe)]Cl_2 complexes (M = Ni, Pd, Pt; dppe = 1,2-(Ph_2P)$_2$$C_2H_4$) at −70 °C affords the M(EH)$_2$Si-heterocyclobutanes **1a**–**d** in moderate yield (Scheme 3). The latter were isolated in the form of orange (**1a**,**b**) and yellow crystals (**1c**–**1d**). Their composition was confirmed by correct combustion analyses (C, H) and mass spectrometry.

The variable temperature ^{1}H- and ^{31}P-NMR spectra of the complexes in C_7D_8 suggest SiME_2-ring inversion

Table 1
Crystallographic data and structure refinement parameters for **1a**, **1c**, **1d**, **3a–b** and **4a–b**

	1a·C_7H_8	**1c**	**1d**	**3a**·C_6H_6	**3b**·C_6H_6	**4a**·$4C_6H_6$	**4b**·$4C_6H_6$
Empirical formula	$C_{52}H_{36}SiP_4Ni$	$C_{45}H_{58}SiP_4Pd$	$C_{45}H_{58}SiP_4Pt$	$C_{51}H_{62}SiP_4Ni$	$C_{51}H_{62}SiP_2As_2Ni$	$C_{92}H_{101}SiP_6Pd_2$	$C_{92}H_{101}SiP_6Ni_2$
Formula weight	871.55	857.33	946.02	885.74	973.64	1633.54	1538.16
Temperature (°C)	203	203	203	203	203	203	298
Crystal system	Triclinic	Monoclinic	Monoclinic	Triclinic	Triclinic	Triclinic	Triclinic
Space group	$P\bar{1}$	$P2_1/c$	$P2_1/c$	$P\bar{1}$	$P\bar{1}$	$P\bar{1}$	$P\bar{1}$
Crystal size (mm)	$0.2\times0.3\times0.5$	$0.3\times0.2\times0.3$	$0.3\times0.2\times0.1$	$0.1\times0.2\times0.2$	$0.2\times0.1\times0.3$	$0.2\times0.3\times0.2$	$0.1\times0.2\times0.2$
Unit cell dimensions							
a (Å)	10.483(5)	12.295(6)	12.271(6)	10.212(5)	10.242(5)	12.778(9)	12.772(3)
b (Å)	13.735(7)	20.24(1)	20.27(1)	14.318(7)	14.200(7)	17.11(1)	17.007(4)
c (Å)	18.576(9)	17.887(9)	17.861(9)	17.291(9)	17.437(9)	22.081(4)	22.449(6)
α (°)	81.50(3)	90	90	83.76(3)	84.10(3)	107.91(4)	107.21(2)
β (°)	75.33(3)	98.72(3)	98.48(3)	79.35(3)	86.21(3)	94.93(4)	94.89(2)
γ (°)	78.06(3)	90	90	75.84(3)	77.48(3)	110.81(4)	110.16(2)
V (Å^3)	2518.58	4400.18	4396.00	2403.82	2460.05	4189.80	4276.16
Z	2	4	4	2	2	2	2
D_{calc} (g cm^{-3})	1.189	1.294	1.429	1.224	1.314	1.295	1.195
Absorption coefficient μ (cm^{-1})	5.7	6.2	33.9	5.9	18.5	6.0	6.1
No. of measured reflections	6593	8002	7888	10508	8663	12424	11135
No. of unique reflections	6591	7750	7638	10484	8663	12424	11131
No. of parameters	512	490	477	531	531	930	916
Θ max (°)	45	50	50	55	50	47	45
Index ranges h, k, l	−10/11, −14/14, 0/19	−14/14, 0/24, 0/21	−14/14, 0/23, 0/21	−12/13, −18/18, 0/22	−12/12, −16/16, 0/20	−14/14, −19/18, 0/24	0/13, −18/17, −24/23
R_1	0.0453	0.0270	0.0342	0.0474	0.0363	0.0312	0.0644
wR_2	0.1135	0.0664	0.0826	0.1289	0.0823	0.0736	0.1655

$R_1 = (\Sigma||F_o|-|F_c||)/\Sigma|F_o|)$ for observed reflections; $wR_2 = \{\Sigma[w(F_o^2-F_c^2]^2)/\Sigma(w(F_o^2)^2\}^{1/2}$ for all measured reflections.

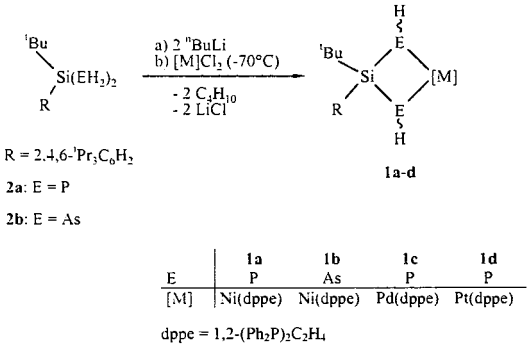

Scheme 3. Synthesis of **1a**–**d**, starting from **2a** and **2b**.

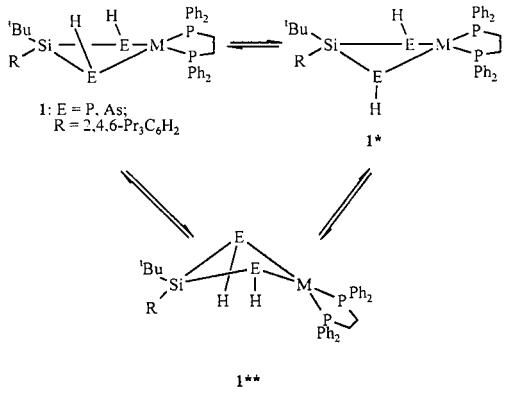

Scheme 4. Dynamic processes of **1** in solution.

and, at the same time, inversion of configuration at the E atoms (E = P, As). Such dynamic processes were also obtained for related 1,3,2,4-$Si_2(EH)_2$ heterocyclobutanes (E = P, As) [8]. The latter exhibit, as expected, high ring flexibility and strongly reduced P/As-inversion barriers in the range of 10–15 kcal mol^{-1} in comparison to the values of PH_3 (35 kcal mol^{-1}) and AsH_3 (38 kcal mol^{-1}), respectively [9]. The ^{31}P-NMR spectra of **1a** and **1c**,**d** consists of two different phosphorus resonance regions which were assigned to the respective P atoms of the dppe ligand and the higher shielded PH ^{31}P nuclei. While each of the spectra of **1a** and **1d** show only a broad set of signals for the two chemically inequivalent sorts of P atoms at room temperature, **1c** exhibits already three broad, superimposed sets of signals for the P atoms of the dppe ligand at $\delta = 35$–40 and, correspondingly, three broad sets of resonances at $\delta = -216$, -225 and -272 for the PH phosphorus atoms. Which configurations are expected in solution? Basically, one expects the presence of the three diastereomeric forms **1**, **1*** and **1****, whereby **1*** is also enantiomeric, as shown in Scheme 4. The isomers can be converted to one another by ring inversion (**1**/**1****), P inversion (**1**/**1***) and coupled processes (**1***/**1****), respectively.

Since the d^8-metal centers M(2 +) in **1** (M = Ni, Pd, Pt) are, as expected, planar tetracoordinate, which was confirmed by X-ray diffraction analysis (see below), the P atoms in **1a**, **1c** and **1d** could represent an AA′XX′ (**1**, **1****) or an ABXY spin system (**1***) (A, B = PH-^{31}P nuclei, X, Y = dppe-^{31}P nuclei). However, our efforts to distinguish the different configurations by means of low-temperature NOESY ^{31}P-NMR experiments, inspection of the ^2J(P, P)-constants and analysis through ^{31}P-NMR simulations were unsuccessful. Tentative assignment of different species in solution was possible in the case of the ^{31}P-NMR spectrum of **1d** at -40 °C, which shows three good resolved multiplets with ^{195}Pt satellites for the P-ring nuclei (P1, P2: $\delta = -209.2$, -217.1 and -257.7) (Fig. 1) and three signals for the corresponding dppe-P nuclei (P3, P4: $\delta = 48.5$, 48.9, 51.1).

Simulations of the multiplet signals for the PH phosphorus centers P1 and P2 (without ^{195}Pt satellites) revealed a relatively large difference between the ^2J(P, P) constants of the signals at $\delta = -209.2$, (^2J(P1, P2) = 37.6 Hz), -257.7 (^2J(P1, P2) = 30.4 Hz) and that at -217.1. (^2J(P1, P2) = 54.4 Hz). Since large magnitudes of ^2J(P, P) constants are diagnostic for *trans* orientation of the respective lone pairs at phosphorus [10], the less intense multiplet at $\delta = -217.1$ with a relatively large ^2J(P1, P2) constant can be assigned to the diastereomeric form **1d*** with δ (P1) = δ (P2). The corresponding almost identical ^2J(P1, P3) and ^2J(P1, P4) constants of 61.5 Hz and ^1J(P, H) = 166.8 Hz for **1d*** are inconspicuous. However, the *cis*-diastereomer **1d**, having the bulky aryl group at silicon in equatorial position, is probably preferred over **1d**** for steric reasons. Thus, the higher populated multiplet at $\delta = -209.2$ is assigned to the diastereomer **1d**. The preference for the latter configuration was confirmed by X-ray diffraction analysis of **1a**–**d**.

3.2. Solid state structures of *1a*, *1c* and *1d*

Only one of the possible diastereomeric forms with all *cis* oriented E–H and *t*-Bu–Si bonds, identical with **1** in Scheme 4, could be crystallized. This is in accordance with ^{31}P-NMR studies of **1d**, which revealed the same configuration prevailing presently in solution at -40 °C. The crystal structures of the $M(EH)_2Si$ heterocyclobutanes **1a**, **1c** and **1d** (E = P; M = Ni, Pd, Pt) were determined and results (see Tables 1 and 2) for **1a** (triclinic, $P\bar{1}$) and the isotypic homologues **1c**,**d** (monoclinic, $P2_1/c$) are depicted in Figs. 2–4.

The four-membered $M(EH)_2Si$ rings are puckered and the bulky aryl group at silicon prefers the exo position. The puckering angles between the Si1E1E2 and E1E2M planes in **1a** (53.05(6)°) versus **1c** (averaged

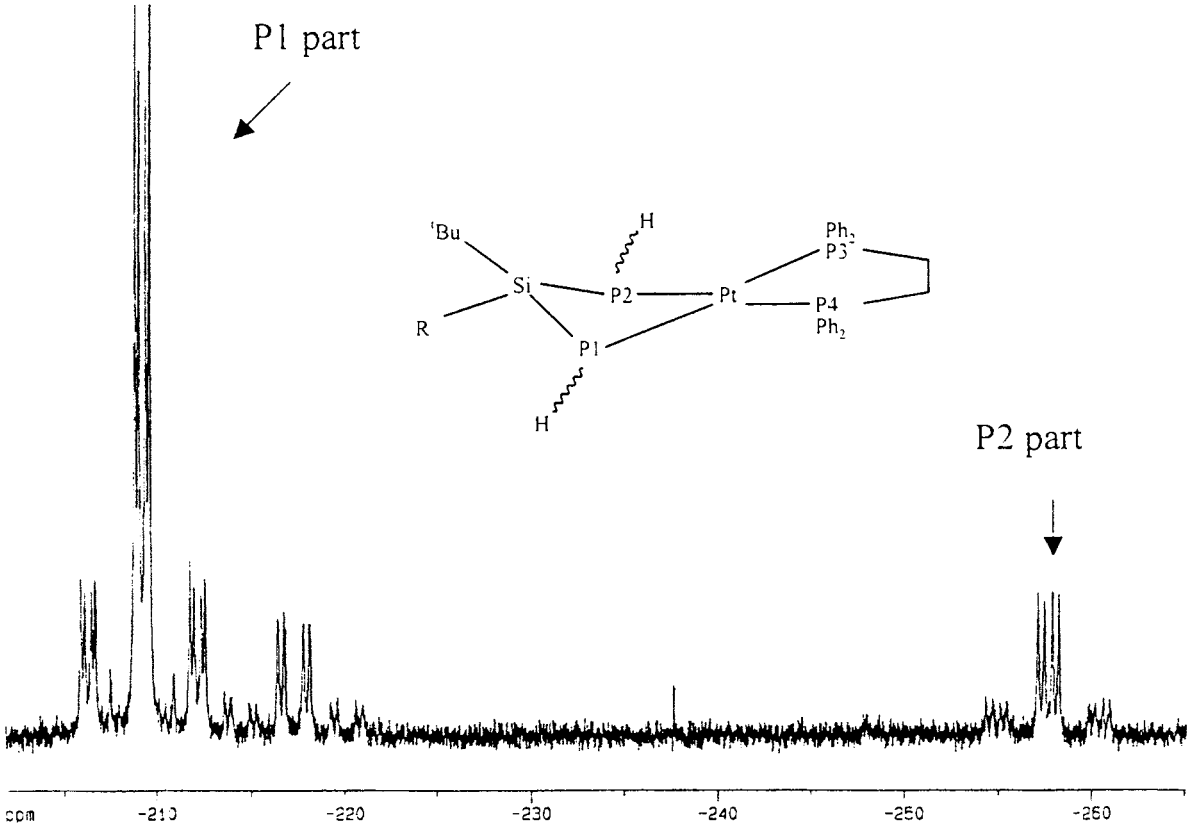

Fig. 1. P1, P2-part of the ^{31}P-NMR spectrum of **1d** in C_7D_8 at -40 °C.

36.3°) and **1d** (36.34(5)°) are significantly different due to the different radii of Ni(2+) versus Pd(+2) and Pt(+2), respectively, but they are larger than the values for related 1,3,2,4-$Si_2(EH)_2$ heterocyclobutanes (E = P, As) [8]. Since the P1 ring atom in **1c** is disordered, but could be refined in two split positions P1A and P1B (Fig. 3), the resulting geometric parameter for the four-membered SiP_2Pd ring are less accurate and deserve no discussion. The H atoms at the pyramidal coordinated P/As atoms are *cis* oriented and the Si atom is distorted tetrahedrally surrounded. While the Si–P, P1–M1 and P2–M1 distances are inconspicuous, the intramolecular P1–P2 distance of 2.91 Å in **1a** is remarkably short. The latter is ca. 0.4 Å shorter than those values observed in 2,4,1,3-$Si_2(PH)_2$ heterocyclobutanes (ca. 3.30 Å) [8], although the Si–P and Ni–P1/Ni–P2 distances are practically equal. This implies that the Ni–P bond is probably less polar than the Si–P bond, which diminishes the repulsive P–P interaction.

The M1–P3 and M1–P4 distances of the dppe-P atoms are shorter than the respective values of the PH phosphorus atoms. The difference is probably due to a higher donor ability of the dppe-P atoms and stronger polarized M–P bonds, despite the fact that P3 and P4 atoms are four-coordinate in contrast to P1 and P2.

*3.3. Synthesis of the NiP_2Si- and $NiAs_2Si$-heterobicyclo[1.1.0]butanes (**3a**,**b**) and the M_2P_2Si-heterobicyclo[1.1.1]pentanes (**4a**,**b**; M = Ni, Pd)*

The one-pot reaction of **2a** with BuLi and [M(dppe)Cl_2] leads at 0 °C instead of -70 °C not only to the Ni$(PH)_2$Si heterocyclobutan (**1a**) but also to

Table 2
Selected bond lengths (Å) and bond angles (°) for **1a**, **1c** and **1d**

	1a [M = Ni]	**1c** [M = Pd]	**1d** [M = Pt]
Bond lengths			
M1–P1	2.264(2)	2.324(8)/2.450(9) [a]	2.383(2)
M1–P2	2.240(2)	2.367(1)	2.371(2)
M1–P3	2.158(1)	2.323(1)	2.286(2)
M1–P4	2.182(2)	2.314(1)	2.279(2)
Si1–P1	2.236(2)	2.243(7)/2.274(a) [a]	2.259(2)
Si1–P2	2.235(2)	2.248(1)	2.252(2)
Bond angles			
Si1–P1–M1	85.42(6)	90.9(3)/87.0(3) [a]	89.46(7)
Si1–P2–M1	86.02(6)	89.66(4)	89.92(7)
P1–Si1–P2	80.82(7)	84.2(4)/90.7(2) [a]	87.10(8)
P1–M1–P2	80.11(6)	79.9(3)/83.8(2) [a]	81.66(6)
P3–M1–P4	88.78(6)	84.93(3)	85.28(5)
Si1–P1–P2/ M1–P1–P2	53.05(6)	43.44(4)/29.21(2)	36.34(5)

[a] The P1 atom has two split positions (P1A/P1B).

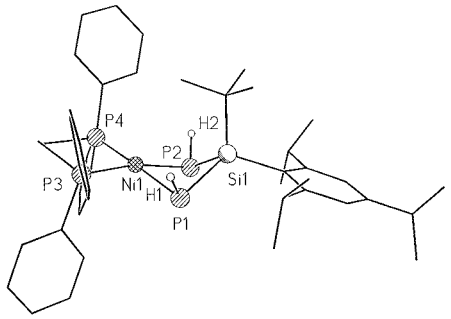

Fig. 2. Solid state structure of **1a**. H atoms were omitted for clarity.

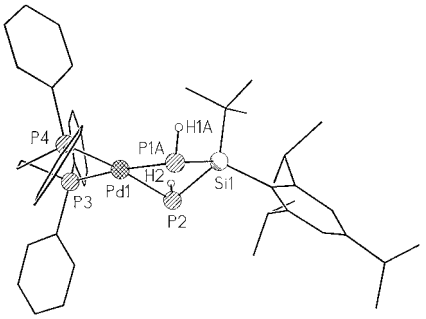

Fig. 3. Solid state structure of **1c**. H atoms were omitted for clarity.

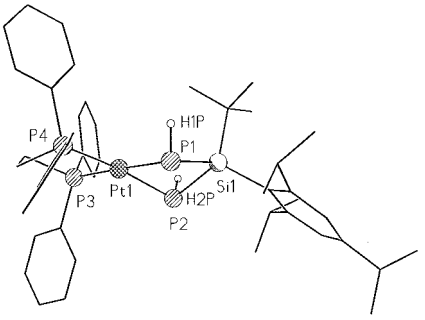

Fig. 4. Solid state structure of **1d**. H atoms were omitted for clarity.

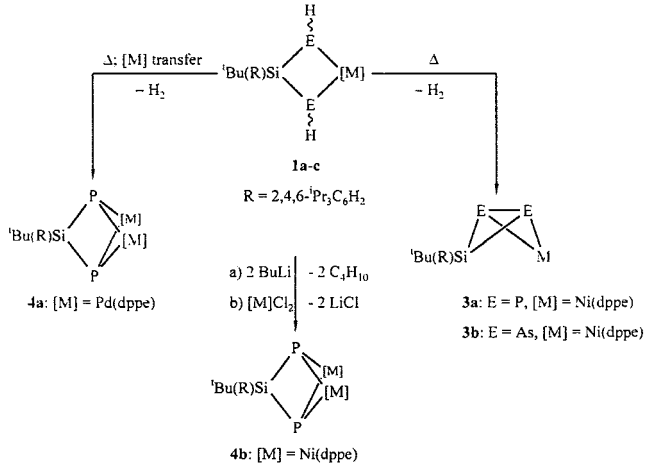

Scheme 5. Synthesis of **3a**,**b** and **4a**,**b**, starting from **1a**–**c**.

the dehydrogenated stereoisomers (*t*-Bu)endo-**3a** and (*t*-Bu)exo-**3a** with P–P bridgehead bonds. The reaction progress and presence of different product isomers can be easily monitored by means of ^{31}P-NMR spectroscopy. While **1a** reveals only one broad signal at $\delta = -190$ for the ring P atoms, the products *t*-Bu(endo)-**3a** and *t*-Bu(exo)-**3a** show each a sharp pseudo triplet signal, corresponding to the respective AA′XX′ spin system (A = ring-P atom, X = dppe-P atom) at $\delta = -82.9$ ((*t*-Bu)endo-**3a**) and -73.8 ((*t*-Bu)exo-**3a**) in the ratio of ca. 5:7:2. Dehydrogenation of residual **1a** to **3a** can be achieved upon heating of the reaction mixture for 8 h in boiling toluene, but only if H_2 is completely removed in the system (Scheme 5).

According to ^{31}P-NMR spectroscopy, a mixture of the isomers (*t*-Bu)endo-**3a** and (*t*-Bu)exo-**3a** results in the ratio of ca. 4:1 which remains unchanged even after heating at higher temperature (130 °C). This proves that ring inversion and configurational isomerization are disfavored. In contrast, P_2Si_2-bicyclo[1.1.1]butanes **A** with different sterically congested exo, endo substituents at silicon can rearrange to the thermodynamic product via rotation of a silandiyl moiety in the transition state [4]. The resulting ratio of isomers of **3a** also reflects the fact that the *t*-Bu-endo isomer **1a** is mainly present in solution from which the preferred formation of (*t*-Bu)endo-**3a** can be easily interpreted. The mechanism of the dehydrogenation of **1a** is hitherto unknown. It has been shown that the conversion of **1a** in toluene into the mixture of isomers of **3a** is concentration-independent (zero order), according to kinetic studies by means of ^{1}H- and ^{31}P-NMR spectroscopy. This suggests that the dehydrogenation occurs in a stepwise intramolecular process, as outlined in Scheme 6: presumably, the reactive intermediate **K** is formed via reductive elimination of [M] and concomitant P–P bond formation. Subsequently, **K** undergoes intramolecular P–H activation through insertion of [M] into a P–H bond and the SiE_2M-butterfly skeleton **3** is finally formed upon H_2 elimination.

Similar mechanisms were already discussed for the formation of diphosphorus (P_2) and diphosphene complexes (RP = PR), starting off from metathesis reactions of silyphosphanes with [(dppe)MCl_2] complexes (M = Ni, Pd, Pt) [11]. While the conversion of the $Si(AsH)_2Ni$ cycles **1b** into the $SiAs_2Ni$-butterfly skeleton in **3b** through As–H activation occurs similarly under relatively mild reaction conditions, the congener $Si(PH)_2M$ cycles **1c** (M = Pd) and **1d** (M = Pt) behave differently. Remarkably, prolonged heating of **1c** in toluene at 80 °C affords the corresponding dipallasiladiphosphabicyclo[1.1.1]pentane derivative **4a** as solely detectable product (^{31}P-NMR) which was isolated in the form of black crystals in 65% yield. This result implies a higher tendency for the hypothetical SiP_2Pd-butterfly skeleton in **3c** to undergo intermolecular [(dppe)Pd] transfer in comparison to the SiP_2Ni-frame

work in **3a**. The thermolysis of **1c** to **4a** can be fully suppressed through addition of 'free' dppe ligand to the solutions. Accordingly, the dehydrogenation of **1a** to **3a** and of **1b** to **3b**, respectively, can also be suppressed upon addition of dppe. This suggests that the rate determining step for the dehydrogenation is strongly influenced by the mobility of the 14 valence electron complex fragments [M]. In contrast to the reactivity of **1a**–**1c**, the $Si(PH)_2Pt$ skeleton in **1d** remains unchanged even if heated in boiling toluene for several days. This implies that the [(dppe)Pt] fragment is surprisingly the least mobile organometallic moiety [M] within the series of compounds, probably because of the higher phosphanido Pt–P bond polarity [12]. An alternative access to dimetallasiladiphosphabicyclo[1.1.1]pentanes is further demonstrated by the two step synthesis of dark red crystalline **4b** in 79% yield, starting off from **1a** via lithiation at phosphorus and salt metathesis reaction with $[Ni(dppe)Cl_2]$. The ^{31}P-NMR spectra of **4a** and **4b** show multiplet pattern of higher order of a AA′BB′XX′ spin system (A,B = dppe-P nuclei, X = phosphido-P nuclei). The spectra prove, as expected, the presence of two planar tetracoordinated M(+2) centers in the M_2P_2Si skeletons in **4a** and **4b**, which was confirmed by X-ray diffraction analysis (see below). The two chemically inequivalent sorts of dppe-P atoms in **4a** and **4b** each show two pairs of multiplets at $\delta = 22.7$, 19.7 and 23.7, 19.4, respectively, and represent the AA′BB′ part of the six spin systems. However, the phosphido-P atoms reveal a broad unresolved signal at $\delta = -80.0$ (**4a**) and -60.5 (**4b**), respectively, and represent the XX′ part of the spin system. Since the latter broad unresolved resonance signals remain even at -30 °C, the spectra simulations revealed useless results.

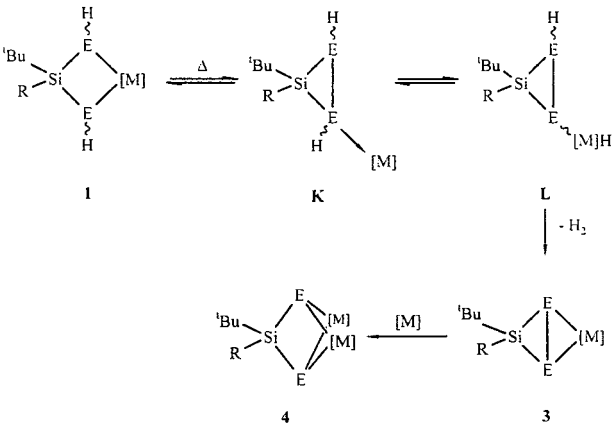

Scheme 6. Proposed mechanism for the intramolecular dehydrogenation of **1** to **3** and rearrangement of **3** to **4**.

Table 3
Selected bond lengths (Å) and bond angles (°) for **3a** and **3b**

	3a (E = P)	**3b** (E = As)
Bond lengths		
Ni1–E1	2.261(1)	2.346(1)
Ni1–E2	2.234(1)	2.353(1)
Ni1–P3	2.164(1)	2.151(1)
Ni1–P4	2.161(1)	2.146(1)
E1–E2	2.223(1)	2.451(1)
Si1–E1	2.224(1)	2.327(1)
Si1–E2	2.215(1)	2.333(1)
Bond angles		
Si1–E1–Ni1	86.77(4)	85.71(4)
Si1–E2–Ni1	87.65(5)	85.43(5)
E1–Si1–E2	60.12(5)	63.46(4)
E1–Ni1–E2	59.30(4)	62.87(4)
P3–Ni1–P4	90.80(4)	91.01(5)
Si1–E1–E2	59.74(4)	58.39(4)
Si1–E2–E1	60.15(4)	58.14(4)
Ni1–E1–E2	59.75(4)	58.69(3)
Ni1–E2–E1	60.95(4)	58.44(4)
Si1–E1–E2/M1–E1–E2	74.84(4)	74.20(4)

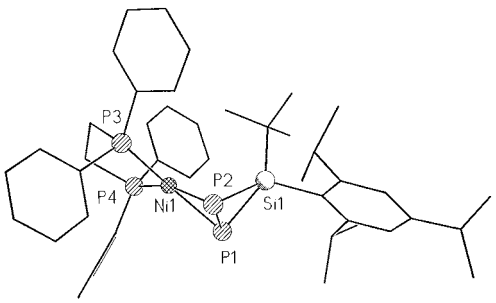

Fig. 5. Solid state structure of **3a**. H atoms were omitted for clarity.

3.4. Molecular structures of (t-Bu)endo-3a and (t-Bu)endo-3b

Single crystals, suitable for X-ray diffraction analysis, could merely be isolated from the respective (*t*-Bu)endo-isomers of **3a** and **3b** in benzene solutions. The isotypical compounds crystallize as benzene-solvates in the triclinic space group $P\bar{1}$. Selected geometric data of the compounds are summarized in Table 3. As expected, the SiE_2Ni skeletons are with 74.8 (**3a**: E = P, see Fig. 5) and 74.2° (**3b**: E = As, see Fig. 6), respectively, stronger puckered than the respective precursors **1a** and **1b**. Compound (*t*-Bu)endo-**3b** represents the first 2,4-diarsametallabicyclo[1.1.0]butane which could be structurally characterized by an X-ray diffraction analysis.

The Ni–P distances of the bridgehead P atoms in endo-**3a** are with 2.261(1) und 2.234(1) Å almost identical and resemble the values observed in analogous butterfly-like Ni_2P_2 complexes [5,11]. However, they are up to 0.1 Å longer than the Ni–P distances with the dppe-P atoms. The Ni–As distances in (*t*-Bu)endo-**3b** (2.346(1), 2.353(1) Å) are only marginally different but, as expected, significantly longer than the values in the dinuclear nickel(+1) arsanido complex $[(Me_3P)NiAs$*t*-

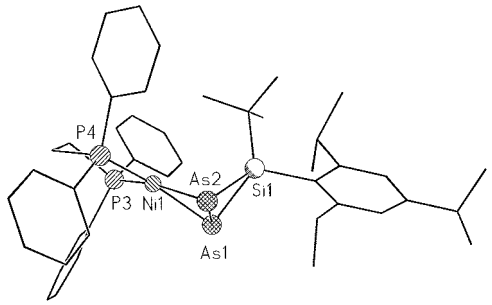

Fig. 6. Solid state structure of **3b**. H atoms were omitted for clarity.

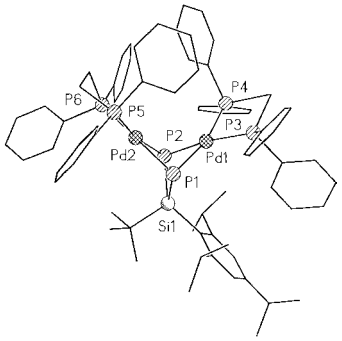

Fig. 7. Solid state structure of **4a**. H atoms were omitted for clarity.

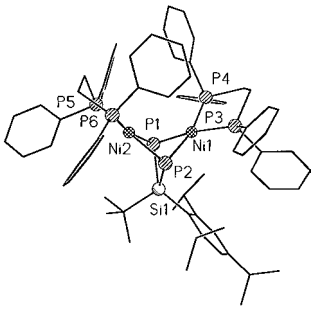

Fig. 8. Solid state structure of **4b**. H atoms were omitted for clarity.

$Bu_2]_2$ (Ni–As 2.27 and 2.26 Å) [13], while the Ni–P distances (2.151(1), 2.146(1) Å) are practically identical with the respective values in (*t*-Bu)endo-**3a**. The E–E distances in (*t*-Bu)endo-**3a** (E = P, 2.23(1) Å) and (*t*-Bu)endo-**3b** (E = As, 2.451(1) Å) are practically identical with the values of unstrained E–E bonds in respective diphosphanes (P–P: 2.22 Å) and diarsanes (As–As: 2.35–2.44 Å). This is remarkable since the E–E distances in Si_2E_2-butterfly skeletons ca. 6% longer, while analogous Ni_2E_2-butterfly derivatives have ca. 5% shorter E–E bridgehead distances [5,13]. Apparently, the nickel atom in the hybridic butterfly-like SiE_2Ni skeletons reduces charge repulsion between the negatively polarized bridgehead E atoms ($Si^{\delta+}$–$E^{\delta-}$–$Ni^{\delta+}$) through its π-acceptor character. This proves that the Ni atom offsets most of the ring strain effects caused by the Si ring atom. The Si–E distances and the endocyclic E1–Si1–E2 and E1–Ni–E2 angles are inconspicuous and little different from those values of related systems [4,5].

3.5. Molecular structures of *4a*,*b*

The isotypical compounds **4a**,**b** crystallize in the space group $P\bar{1}$ and have an asterane-like SiP_2M_2 skeleton at which neither the P–P distances of 3.00 (**4a**, see Fig. 7) and 2.84 Å (**4b**, see Fig. 8), respectively, nor the M–M distances (3.02 (**4a**) and 2.89 Å (**4b**)) suggest any favorable P–P- and M–M-σ interactions, respectively. The SiM_2P_2 skeletons are isostructural with that of the currently reported Si_2P_2Pt skeleton in a platinadiphosphadisilabicyclo[1.1.1]pentane which has a P–P distance of 3.063(7) Å [14]. The pyramidally λ^3-coordinated phosphorus atoms and the almost equidistant M1–P1, M1–P2, M2–P1 and M2–P2 distances in **4a** and **4b** reflect the expected electronic features for metal phosphido complexes of that type. Selected distances and angles for **4a**,**b** are summarized in Table 4.

As expected, the metal(+2) centers are tetragonal-planar coordinate and the respective M–P distances for the dppe-P atoms are significantly shorter. The Si–P distances in **4a** and **4b** show only marginally differences but lead to relatively acute endocyclic P–Si–P angles of 83.87(6) (**4a**) and 79.15(8)° (**4b**), respectively. Similarly, the endocyclic P1–M1–P2 and P1–M2–P2 angles in **4a** and **4b** are also almost identical. However, the latter are in **4a** ca. 6° but in **4b** only ca. 0.9° smaller than the respective P1–Si1–P2 angle. Apparently, this reflects geometric restrictions and minimizes ring strain. The

Table 4
Selected bond lengths (Å) and bond angles (°) for **4a** and **4b**

	4a (M = Pd)	**4b** (M = Ni)
Bond lengths		
M1–P1	2.394(1)	2.259(2)
M1–P2	2.387(1)	2.259(2)
M2–P1	2.385(1)	2.248(2)
M2–P2	2.379(1)	2.255(2)
M1–P3	2.329(1)	2.216(2)
M1–P4	2.309(1)	2.185(2)
M2–P5	2.330(1)	2.202(2)
M2–P6	2.328(1)	2.200(2)
Si1–P1	2.244(2)	2.234(2)
Si1–P2	2.247(1)	2.229(2)
M1–M2	3.026(1)	2.890(1)
Bond angles		
Si1–P1–M1	83.87(6)	85.29(7)
Si1–P1–M2	86.97(6)	87.35(7)
M1–P1–M2	78.59(4)	79.74(6)
P1–Si1–P2	83.44(6)	79.15(8)
P1–M1–P2	77.38(5)	78.01(6)
P1–M2–P2	77.72(5)	78.31(6)
P3–M1–P4	84.63(2)	86.60(7)

M–P distances are inconspicuous and practically identical with the values in **1a**, **1c** and **3a**, respectively (see Tables 2 and 3).

4. Supporting material

Crystallographic data for the structural analysis have been deposited with the Cambridge Crystallographic Data Centre, CCDC nos. 164584–164590 for compounds **1a**, **1c**, **1d**, **3a**, **3b**, **4a** and **4b**, respectively. Copies of this information may be obtained free of charge from The Director, CCDC, 12 Union Road, Cambridge CB2 1EZ, UK (Fax: +44-1223-336033; e-mail: deposit@ccdc.cam.ac.uk or www: http://www.ccdc.cam.ac.uk).

Acknowledgements

We are grateful to the Deutsche Forschungsgemeinschaft, the Fonds der Chemischen Industrie and the Ministerium für Schule, Wissenschaft und Forschung des Landes Nordrhein-Westfalen for financial support.

References

[1] (a) R.S. Grev, H.F. SchaeferIII III, J. Am. Chem. Soc. 109 (1987) 6569;
(b) P.v.R. Schleyer, in: H.G. Viehl, R. Janoschek, R. Merenyi (Eds.), Substituent Effects in Radical Chemistry, Reidel, Dordrecht, 1986, p. 69;
(c) Review: Y. Apeloig, Theoretical Aspects of Organosilicon Compounds, in: S. Patai, Z. Rappoport (Eds.), The Chemistry of Silicon Compounds, Part 1, Wiley, New York, 1989, p. 89ff;
(d) D.B. Kitchen, J.E. Jackson, L.C. Allen, J. Am. Chem. Soc. 112 (1990) 3408;
(e) S. Nagase, Polyhedron 10 (1991) 1299.

[2] (a) J.A. Boatz, M.S. Gordon, J. Phys. Chem. 92 (1988) 3037;
(b) W. Kutzelnigg, Angew. Chem. 96 (1984) 262; Angew. Chem. Int. Ed. Engl. 23 (1984) 272;
(c) R. Janoschek, Chem. Unserer Zeit 21 (1988) 128;
(d) W.W. Schoeller, T. Dabisch, Inorg. Chem. 26 (1987) 1081.

[3] (a) S. Masamune, Y. Kabe, S. Collins, D.J. Williams, R. Jones, J. Am. Chem. Soc. 107 (1985) 5552;
(b) R. Jones, D.J. Williams, Y. Kabe, S. Masamune, Angew. Chem. Int. Ed. Engl. 25 (1986) 173;
(c) T. Kawase, S.A. Batcheller, S. Masamune, Chem. Lett. (1987) 227;
(d) M. Kira, T. Iwamoto, C. Kabuto, J. Am. Chem. Soc. 118 (1996) 10303;
(e) T. Iwamoto, M. Kira, Chem. Lett. (1998) 277.

[4] (a) M. Driess, A.D. Fanta, D.R. Powell, R. West, Angew. Chem. Int. Ed. Engl. 28 (1989) 1038;
(b) M. Driess, H. Pritzkow, M. Reisgys, Chem. Ber. 124 (1991) 1923;
(c) A.D. Fanta, R.P. Tan, N.M. Comerlato, M. Driess, D.R. Powell, R. West, Inorg. Chim. Acta 198–200 (1992) 733;
(d) M. Driess, R. Janoschek, H. Pritzkow, Angew. Chem. Int. Ed. Engl. 31 (1992) 460;
(e) M. Driess, H. Pritzkow, S. Rell, R. Janoschek, Inorg. Chem. 36 (1997) 5212.

[5] (a) H. Schäfer, D. Binder, D. Fenske, Angew. Chem. Int. Ed. Engl. 24 (1985) 522;
(b) H. Schäfer, D. Binder, Z. Anorg. Allg. Chem. 546 (1987) 55;
(c) Reviews: O.J. Scherer, Acc. Chem. Res. 32 (1999) 751;
(d) K.H. Whitemire, Adv. Organomet. Chem. 42 (1998) 1.

[6] M. Driess, H. Pritzkow, M. Reisgys, Chem. Ber. 124 (1991) 1931.

[7] M. Driess, H. Pritzkow, Chem. Ber. 127 (1994) 477.

[8] (a) M. Baudler, H. Jongebloed, Z. Anorg. Allg. Chem. 458 (1979) 9;
(b) M. Baudler, T. Pontzen, Z. Anorg. Allg. Chem. 491 (1982) 27;
(c) G. Fritz, Adv. Inorg. Chem. 31 (1987) 171;
(d) G. Fritz, R. Biastoch, Z. Anorg. Allg. Chem. 535 (1986) 63 (see also [6]).

[9] (a) S. Nagase, General and Theoretical Aspects, in: S. Patai (Ed.), The Chemistry of Organic Arsenic, Antimony and Bismuth Compounds, Wiley, New York, 1994, p. 1 (and cited references therein);
(b) Review: D.G. Gilheany, Chem. Rev. 94 (1994) 1339;
(c) M. Driess, K. Merz, C. Monsé, Z. Anorg. Allg. Chem. 626 (2000) 2264.

[10] J. Hahn, Higher Order Spectra of Polyphosphorus Compounds, in: J.G. Verkade, L.D. Quin (Eds.), Phosphorus-31 NMR Spectroscopy in Stereochemical Analysis, VCH, Weinheim, 1987, p. 348.

[11] H. Schäfer, D. Binder, Z. Anorg. Allg. Chem. 560 (1988) 65 (and references cited therein; see also [5]).

[12] D.K. Wicht, S.N. Paisner, B.M. Lew, D.S. Glueck, G.P.A. Yap, M. Liable-Sands, A.L. Rheingold, C.M. Haar, S.P. Nolan, Organometallics 17 (1998) 652.

[13] R.A. Jones, B.R. Wittlesy, Inorg. Chem. 25 (1986) 852.

[14] A.D. Fanta, M. Driess, D.R. Powell, R. West, J. Am. Chem. Soc. 113 (1991) 7806.